



**Fermilab**

TM-1388  
0401.000

AN ESTIMATE OF THE LONGITUDINAL AND TRANSVERSE IMPEDANCES  
OF THE MAIN RING IN THE TEV I PROJECT

K.-Y. Ng

February 1986

AN ESTIMATE OF THE LONGITUDINAL AND TRANSVERSE  
IMPEDANCES OF THE MAIN RING IN TEV I PROJECT

King-Yuen Ng

February 1986

I. INTRODUCTION

Although the Fermilab Main Ring was built 15 years ago its longitudinal and transverse impedances have never been estimated. This is because the Main Ring was formerly used as a fixed target machine which required large longitudinal phase space in order to achieve a better duty cycle. In fact, the phase space was blown up deliberately by a bunch spreader. Microwave instability would further increase the phase space due to overshooting. As a result, the issue of impedances has never been brought up.

However, in Tevatron I, the functions of the Main Ring are quite different. The Main Ring has to accelerate intense bunches of protons and antiprotons for collision in the Energy Saver. As a result, the phase space area of each bunch has to be carefully controlled in order to arrive at a high luminosity during collision. Before extraction, both the proton and antiproton bunches undergo a coalescence procedure, during which the energy spread of the bunches is reduced to a minimum and therefore instabilities can occur. Similar RF maneuvering is also required before extracting

the proton bunches at 120 GeV for antiproton production. Therefore, to guarantee the successful performance of the Main Ring in Tevatron I, its stability limits and impedances have to be estimated and controlled. The limits for some single bunch instabilities in different Main Ring functions have been computed in Reference 1. In this note, we try to estimate the impedances of the Main Ring.

## II. BELLOWS

The main contribution to the impedances may come from the bellows. A typical bellow is shown in Figure 1. It consists of a pill-box cavity of length  $l \sim 15.85$  cm and radius  $d \sim 7.16$  cm with only four to five ripples at one end and a porthole connected to the vacuum pump. A bellow of such size is necessary because it has to join the 1.5 in x 5 in rectangular beam pipes of the B1 magnets, the 2 in x 4 in rectangular beam pipes of the B2 magnets, the  $\sim 3.8$  cm x 6 cm rhombic beam pipes of the quadrupoles and also some circular beam pipes of the straight sections. For such a bellow, the main contribution will come from the narrow resonances of the pill box rather than the ripples. We try to run the code<sup>2</sup> TBCI on the bellow by assuming that the beampipes on both sides are circular and are of radius  $b \sim 3.61$  cm. This corresponds to a cutoff frequency of 3.18 GHz for the TM mode and is roughly the lowest TM-mode cutoff frequency for

all the various beam pipes. A Gaussian test bunch of RMS length 4 mm is used and the monopole wake field (Figure 2) is truncated at 80 cm. The real and imaginary parts of the longitudinal impedance are shown in Figures 3 and 4 respectively. We see that there are four narrow resonances before cutoff; they correspond to the resonances of the pill-box cavity itself. Above cutoff, there are small resonances with a spacing of  $\sim 0.95$  GHz; they correspond to waves bouncing back and forth between the end plates of the cavity. We also run the code for bellow with all ripples removed. The results are very similar with the exception that the resonances are shifted a little bit upward in frequency. The bellow is next analyzed in the frequency domain using the code<sup>3</sup> URMEL, from which the quality factors  $Q$  and  $R/Q$  of the narrow resonance are obtained and are listed in Table I. The  $R/Q$  of the first resonance is very small. This is the result of the transit-time effect. The longitudinal electric field of this mode does not vary very much from one end to the other end of the bellow. However, this field just changes sign as the particle reaches the middle of the bellow, and therefore a near complete cancellation takes place.

There are roughly 1000 bellows in the Main Ring. They are not exactly identical and therefore spreads in

resonance frequencies are anticipated. The bellows (about 130 pieces) from E25 to F25 have been measured by Jim Crisp; the radii and lengths have standard deviations  $\Delta b/b = 0.00317$  and  $\Delta \ell/\ell = 0.0342$  respectively. The first four resonances correspond to the  $TM_{01p}$  modes with  $p = 0, 1, 2, 3$ . With the radius of the attached beampipe reduced to zero, their resonance frequencies will be

$$f = \sqrt{\left(\frac{2.405}{a}\right)^2 + \left(\frac{p\pi}{\ell}\right)^2}, \quad (2.1)$$

with which the spreads in frequencies can be estimated. Taking these spreads to be Gaussian, the actual shapes of the four resonances for the sum of 1000 bellows can be computed. The shunt impedances and  $Q$  are listed in Table I. Also listed are the widths of the resonances in standard deviations  $\sigma_\omega$  as well as  $Z_{11}/n$  at the peaks. We see that  $Z_{11}/n$  are of order 14.7 to 78.7  $\Omega$ . However, the widths  $\sigma_\omega = 0.023$  to 0.36 GHz are very small too. In fact, they are very much smaller than the width of the spectrum of a bunch, which cannot be less than  $\sigma_\tau^{-1} = 0.26$  GHz, because the RMS bunch length when multiplied by  $2\sqrt{6}$  cannot be bigger than 18.8 ns, the maximum width of a bucket. Thus, what a bunch sees is not the peak  $Z_{sh}$  of the resonance, but only an effective shunt impedance  $Z_{sh}\sigma_\omega\sigma_\tau$ , after averaging over the

bunch spectrum. Since this quantity depends on the length of a bunch, it is not a handy quantity to quote. In fact,  $Z_{sh}/Q$  is the quantity we need when the width of the resonance is less than the width of the bunch spectrum, because the microwave limit for such a situation can be written as

$$\frac{Z_{sh}}{Q} < \frac{4|\eta|(E/e)\left(\frac{\sigma_E}{E}\right)^2}{I_{AV}}, \quad (2.2)$$

where  $\eta$  is the frequency dispersion parameter,  $E$  the particle energy,  $\sigma_E$  the RMS energy spread and  $I_{AV}$  the average bunch current. We want to point out that Eq. (2.2) has never been proved vigorously<sup>4</sup>. The limits in each stage of the functions of the Main Ring are given in Tables II, III and IV. The worst limit is  $Z_{11}/Q = 4.1 \text{ k}\Omega$  which occurs in the preparation of the proton bunch for antiproton production, when the RF voltage is reduced to  $\sim 117 \text{ kV}$  within two turns at the 120 GeV flat top and the bunch is allowed to shear to a length that fills nearly one half of the bucket. During the coalescence of proton and antiproton bunches, the lowest stability limits are  $\sim 19 \text{ k}\Omega$  and  $28 \text{ k}\Omega$  respectively. On the other hand, one thousand bellows will provide for the first four resonances  $Z_{sh}/Q = 2.4 \text{ k}\Omega$ ,  $37 \text{ k}\Omega$ ,  $24 \text{ k}\Omega$  and  $29 \text{ k}\Omega$ . Therefore, microwave instability is

inevitable. To ensure stability, these pill-box bellows must be shielded.

The bellows are also examined in the dipole modes using URMEL, (TBCI cannot be used in the dipole mode for a wake longer than ~80 cm since an instability occurs in the code). Narrow resonances are seen. The transverse impedances  $Z_{\perp}$  over  $Q$  can be obtained using the formula

$$\frac{Z_{\perp}}{Q} = \frac{c}{\omega_R r_o^2} \cdot \frac{Z}{Q}, \quad (2.3)$$

where  $r_o$  is the radius of the beam pipe where the longitudinal  $Z/Q$  is computed. The results are listed in Table V. The largest contribution is  $Z_{\perp}/Q = 0.26 \text{ M}\Omega/\text{m}$  for 1000 bellows at 2.50 GHz. For resonances with width less than the spectral width of the bunch, a stability limit, similar to Eq. (2.2), can be given for the transverse microwave or fast head-tail instability:

$$\frac{Z_{\perp}}{Q} < 8\sqrt{\frac{2}{\pi}} \frac{|\eta|(E/e)(\sigma_E/E)}{I_{AV} \bar{\beta}}, \quad (2.4)$$

where  $\bar{\beta}$  is the average beta-function. The worst limits for preparation of  $\bar{p}$  production,  $p$ -bunch coalescence and  $\bar{p}$ -bunch coalescence are 5.5, 13 and 20  $\text{M}\Omega/\text{m}$  respectively (see Tables II, III and IV). Therefore, fast head-tail is safe.

Different oscillation modes of a single bunch can be mixed and instabilities slow compared with the synchrotron frequency can occur. These instabilities are driven by  $|\bar{Z}_{11}/n|$  and  $|\bar{Z}_\perp|$  at low frequencies. The worst limits for preparation of  $\bar{p}$  production, p-bunch coalescence and  $\bar{p}$ -bunch coalescence are  $|\bar{Z}_{11}/n| = 7.2, 39, \text{ and } 58 \Omega$  respectively and  $|\bar{Z}_\perp| = 6.2, 15, \text{ and } 22 \text{ M}\Omega/\text{m}$ . The contributions of the 1000 bellows are, from TBCI,  $\text{Im } \bar{Z}_{11}/n = 2.46 \Omega$  and from the theoretical estimation<sup>5</sup>,

$$\text{Im } \bar{Z}_\perp \approx \frac{Z_0}{\pi d} \frac{(d/b - 1)^2}{0.45 + 0.39 d/b} \times 1000 = 1.32 \text{ M}\Omega/\text{m}. \quad (2.5)$$

Thus, these instabilities will not be driven by the bellows.

### III. BEAM POSITION MONITORS

There are about  $M = 200$  beam position monitors in the Main Ring. As shown in Figure 5, they are rectangular in shape,  $\ell = 11.75 \text{ cm}$  in length, slant cut diagonally and terminated at the center by a resistance 50 ohms. If we approximate each monitor to be circular in cross section with an open angle  $2\phi_0 \sim \pi$  for each half and also the termination is matched to the characteristic impedance  $Z_c$ , the longitudinal impedance at low frequencies is given by

$$\frac{Z_{||}}{n} = 2MZ_c \left(\frac{\phi_0}{\pi}\right)^2 \frac{\ell}{R} \left(\frac{n\ell}{R} + j\right), \quad (3.1)$$



where  $R$  is the radius of the Main Ring. We get

$$\frac{Z_{||}}{n} = (6.91 \times 10^{-5} n + j 0.588) \Omega \quad (3.2)$$

for  $n \ll 1.7 \times 10^4$  or  $\omega/2\pi \ll 2.6$  GHz. The transverse impedance is approximately given by

$$Z_{\perp} \approx \frac{2R}{b^2} \frac{Z_{||}}{n} = (1.06 \times 10^{-4} n + j 0.902) M\Omega/m. \quad (3.3)$$

These impedances are safe against slow single bunch instabilities.

Because these monitors are terminated at the center, resonances can occur at  $f = mc/2\ell$ ,  $m = 1, 2, \dots$ , for both the longitudinal and transverse cases. Thus the lowest resonance is at  $f = 1.28$  GHz. The shunt impedances and quality factors of these resonances are

$$Z_{sh} = Z_c^2 \frac{2\pi b \sigma \delta}{\ell},$$

$$Q = \tau / \delta, \quad (3.4)$$

where

$$\tau = \frac{2\pi b Z_c}{Z_o}$$

is the electrical equivalent distance between the monitor and ground,  $Z_c$  the characteristic impedance,  $\delta$  the skin depth,  $\sigma$  the conductivity of the monitor and  $Z_0 = 377$  ohms. Taking  $b = 3.61$  cm,  $Z_c = 50$  ohms, we get  $\tau = 3.00$  cm. Taking  $\sigma = 0.14 \times 10^7$  mho/m, we get for 200 monitors  $Z_{sh}/Q = 6.38 \text{ m}^{-1} \text{ k}\Omega$  and  $Q = 2520 \text{ m}^{1/2}$ . The transverse impedance can be estimated from Eq. (2.3). The result is  $Z_{\perp}/Q = 0.183 \text{ m}^{-2} \text{ M}\Omega/\text{m}$ . Comparing with the limits in Table II, it is evident that longitudinal microwave growth can be driven by these resonances. However the fast head-tail is safe. To safeguard stability, these resonances should be eliminated by terminating the monitors at the ends rather than the center.

#### IV. WALL RESISTIVITY

The vacuum chamber of the Main Ring consists of beam pipes of different cross sections. They include:

- a) 7560 ft. of 1.5"x5" rectangular beam pipe inside 378 B1 dipoles and 7920 ft. of 2"x4" rectangular beam pipe inside 39 B2 dipoles,
- b) 1344 ft. of rhombic beam pipe inside 192 7-ft. quads and 192 ft. of rhombic beam pipe inside 48 4-ft. quads (the rhombic pipe will be approximated by circular pipe of radius 3.8 cm),
- c) 576 ft. of 1.5"x5" rectangular pipe and 576 ft. of 2"x4" rectangular pipe in the straight sections,

d) 624 ft. of 6 in. circular pipe, and

e) 188.75 ft. of 5 in. circular pipe in the RF region.

The pipe in the RF region is of copper while the rest is stainless steel. Exact formulas for circular and rectangular pipes are available<sup>6</sup>. The total contributions are

$$\frac{Z_{||}}{n} = (1+j) 14.5 n^{-\frac{1}{2}} \Omega,$$
$$Z_{\perp} = \begin{cases} (1+j) 50.5 n^{-\frac{1}{2}} \text{ M}\Omega/\text{m}, & (\text{vertical}) \\ (1+j) 25.8 n^{-\frac{1}{2}} \text{ M}\Omega/\text{m}. & (\text{horizontal}) \end{cases}$$

These impedances will be too small in the microwave region to cause any fast instability. Slow growths are driven by the average impedances seen by the bunch. The longest bunch is the one that fills the bucket, of  $\sigma_T = 18.8/2\sqrt{6} = 3.72$  ns. The average impedances are then  $\text{Im } \bar{Z}_{||}/n = 1.01$  ohm and  $\text{Im } \bar{Z}_{\perp} = 3.51$  M $\Omega/\text{m}$  for vertical and 1.79 M $\Omega/\text{m}$  for horizontal. They are well below the theoretical limits.

## V. KICKERS AND LAMBERTSONS

The Main Ring contains extraction kickers for transferring protons and antiprotons to the Energy Doubler

and protons for  $\bar{p}$ -production, abort kicker for proton and also injection kickers for transferring protons from the booster and antiprotons from the accumulators. These kickers are of the form of window magnets either of size 2"x6" and length  $\ell = 1$  m or 1 1/2" x 3 3/8" and length  $\ell = 1.9$  m. The longitudinal and transverse impedances of these kickers have been estimated by Nassibian and Sacherer<sup>7</sup>. At low frequencies, they are

$$\frac{Z_{||}}{n} = \frac{Z_0 x_0^2 \ell}{AR},$$

$$Z_{\perp} = \frac{Z_0 \ell}{A},$$

where A is the area of the magnet cross section, R the ring radius and  $x_0$  the displacement of the beam from the center of the magnet. Our result gives  $Z_{11}/n = 0.033 \Omega$  and  $Z_{\perp} = 0.87 \text{ M}\Omega/\text{m}$ .

There are eight Lamberstons in the Main Ring, each of length 10 ft. The impedances of a Lambertson have been estimated before<sup>8</sup>. In our case, below  $\sim 0.5$  GHz,

due to the flow of image current around the magnet laminations. When averaged over the bunch spectrum, we get  $\text{Im}\bar{Z}_{11}/n = 0.23 \Omega$  and  $\text{Im}\bar{Z}_{\perp} = 0.52 \text{ M}\Omega/\text{m}$ . For higher frequencies, there are broad resonances with  $Q \sim 3$  to 10. This first resonance is at  $\sim 1$  GHz with  $Z_{11}/n = 2.1 \Omega$  and  $Z_{\perp} = 0.47 \text{ M}\Omega/\text{m}$  at the peak. The estimations in Reference 8 have been checked experimentally by making measurement with a hook-up wire in place of the beam. The experimental results suggest values that are roughly  $\sim 5$  times smaller than the estimated ones at low frequencies. If this is true also in the resonance region, the resonances may not be able to drive an instability even in the worst situation when the RF voltage is lowered to prepare the proton bunch for  $\bar{p}$ -production. Otherwise, the laminations in the Lambertsens have to be shielded.

## VI. SUMMARY

The estimations of all the contributions to the longitudinal and transverse impedances are listed in Table VI and plotted in Figures 6 and 7. The stability limits for the worst situation are also listed in Table VI for comparison. We see that the slow-growing single bunch instability caused by longitudinal mode coupling is safe. But the corresponding instability caused by transverse mode coupling is not (at least for the vertical). As for the

fast-growing longitudinal microwave instability, it can be driven by the sharp resonances of the bellows and beam monitors and may be the broad resonances of the Lambertsens also. However, the fast-growing transverse microwave instability (fast head-tail) is safe. To have stability, the bellows have to be shielded and the beam monitors terminated at the ends instead of the center. The slow-growing transverse mode coupling can be cured by feed-back.

#### VII. REFERENCES

1. K.Y. Ng, Fermilab Report TM-1383
2. T. Weiland, DESY 82-015, 1982
3. T. Weiland, DESY M-82-24, 1982
4. If we include only the real part of the impedance and let  $Q$  tend to infinity, Eq. (2.2) follows immediately. However, the neglect of the imaginary part which carries a long tail is a violation of causality.
5. K.Y. Ng, Fermilab Report, FN-389
6. K.Y. Ng, Particle Accelerators 16, 63 (1984)
7. G. Nassibian and F. Sacherer, CERN/ISR-TH/77-61
8. K.Y. Ng, Fermilab Report, UPC-149.

Table I. Longitudinal impedance of the resonances of bellows

Resonance frequency (GHz)	For 1 bellow		For 1000 bellows			
	Z/Q ( $\Omega$ )	Q	$Z_{sh}/n$ ( $\Omega$ )	Q	$\sigma_\omega$ (GHz)	$\sigma_\omega^{-1}$ (ns)
1.57	2.378	4908	19.3	266	0.023	43.1
1.84	36.94	4018	78.7	82	0.088	11.3
2.42	24.25	4415	20.6	43	0.222	4.5
3.14	28.85	4597	14.7	34	0.349	2.7

Note: Column 1 is from TBCI for bellow with ripples.  
Column 2 is from URMEL for bellow without ripples.  
Column 3 is for stainless steel with  $\sigma = 0.14 \times 10^7$  mho/m.  
Column 6:  $\sigma_\omega$  is the equivalent RMS Gaussian width with  $\sqrt{2\pi}\sigma_\omega = \pi^2 f_R / Q$ .

Table II. RF maneuvering of proton bunches for  $\bar{p}$  production

	120 GeV flat top	$V_{RF}$ reduced and bunch rotates to max time spread	$V_{RF}$ raised to 4 MV bunch rotates for $90^\circ$
Longitudinal emittance $6\pi\sigma_z^2\sigma_E^2$	0.1 eV-sec	0.1 eV-sec	0.1 eV-sec
$\sqrt{\delta\sigma_z^2}$	.78 ns	4 ns	0.5 ns
$\sqrt{\delta\sigma_E^2} (\sqrt{\delta\sigma_E^2}/E)$	49.1 MeV ( $4.06 \times 10^{-4}$ )	6.98 MeV ( $5.77 \times 10^{-5}$ )	239 MeV ( $1.98 \times 10^{-3}$ )
$V_{RF}$	4 MV	117 kV	4 MV
Bucket height	314 MeV	53.7 MeV	314 MeV
$\gamma_s$	0.00405	0.000693	0.00405
Number per bunch	$2.4 \times 10^{10}$	$2.4 \times 10^{10}$	$2.4 \times 10^{10}$
Fast growth limits			
broad band $Z_H/n$	12.2 $\Omega$	1.27 $\Omega$	186 $\Omega$
$Z_L$	73.4 M $\Omega$ /m	53.5 M $\Omega$ /m	229 M $\Omega$ /m
narrow res. $Z_H/Q$	201 k $\Omega$	4.06 k $\Omega$	4.76 M $\Omega$
$Z_L/Q$	39.0 M $\Omega$ /m	5.55 M $\Omega$ /m	190 M $\Omega$ /m
Slow growth limits			
$\bar{Z}_H/n$	69.0 $\Omega$	7.18 $\Omega$	1050 $\Omega$
$\bar{Z}_L$	43.4 M $\Omega$ /m	6.16 M $\Omega$ /m	211 M $\Omega$ /m

Note: The fast growth broad band limits of  $Z_L$  are computed at 1.5 GHz



Table III. Coalescence of 7 proton bunches at 150 GeV

	Start	$V_{RF}$ lowered to match bunch	7 bunches in $h=53$ bucket	End of 90° rotation	Recapture into $h=1113$ bucket	$V_{RF}$ increases before extraction
Longitudinal emittance $6\pi\sigma_z^2\sigma_E$	0.20 eV-sec	0.20 eV-sec	1.39 eV-sec	2.19 eV-sec	1.45 eV-sec	1.45 eV-sec
$\sqrt{6}\sigma_z$	1.63 ns	9.4 ns	65.8 ns	8.89 ns	9.4 ns	3.99 ns
$\sqrt{6}\sigma_E$ ( $\sqrt{6}\sigma_E/E$ )	39.0 MeV ( $2.60 \times 10^{-4}$ )	8.31 MeV ( $5.54 \times 10^{-5}$ )	8.31 MeV ( $5.54 \times 10^{-5}$ )	61.5 MeV ( $4.10 \times 10^{-4}$ )	60.3 MeV ( $4.02 \times 10^{-4}$ )	116 MeV ( $7.7 \times 10^{-4}$ )
$V_{RF}$	0.68 MV	2.30 kV	22 kV	22 kV	0.12 MV	1.0 MV
$h$	1113	1113	53	53	1113	1113
$\gamma_s$	$1.51 \times 10^{-3}$	$8.72 \times 10^{-5}$	$5.91 \times 10^{-5}$	$5.91 \times 10^{-5}$	$6.37 \times 10^{-4}$	$1.83 \times 10^{-3}$
Number per bunch	$1.2 \times 10^{10}$	$1.2 \times 10^{10}$	$8.4 \times 10^{10}$	$8.4 \times 10^{10}$	$8 \times 10^{10}$	$8 \times 10^{10}$
Fast growth limits						
broad band $Z_{  }/n$	$26.2 \Omega$	$6.86 \Omega$	$6.86 \Omega$	$50.8 \Omega$	$54.2 \Omega$	$84.4 \Omega$
$Z_{\perp}$	$244 M\Omega/m$	$244 M\Omega/m$	$244 M\Omega/m$	$382 M\Omega/m$	$265 M\Omega/m$	$265 M\Omega/m$
narrow res. $Z_{  }/Q$	$206 k\Omega$	$9.40 k\Omega$	$9.40 k\Omega$	$73 k\Omega$	$73 k\Omega$	$272 k\Omega$
$Z_{\perp}/Q$	$62.0 M\Omega/m$	$13.2 M\Omega/m$	$13.2 M\Omega/m$	$14.0 M\Omega/m$	$14.3 M\Omega/m$	$27.7 M\Omega/m$
Slow growth limits						
$\bar{Z}_{  }/n$	$148 \Omega$	$38.8 \Omega$	$38.8 \Omega$	$287 \Omega$	$307 \Omega$	$477 \Omega$
$\bar{Z}_{\perp}$	$68.9 M\Omega/m$	$14.7 M\Omega/m$	$14.7 M\Omega/m$	$15.5 M\Omega/m$	$16.0 M\Omega/m$	$30.7 M\Omega/m$

Note: The fast growth broad band limits of  $Z_{\perp}$  are computed at 1.5 GHz

Table IV. Coalescence of 13 antiproton bunches at 150 GeV

	Start	V <sub>RF</sub> lowered to match bunch	13 bunches in h=53 bucket	End of 90° rotation	Recapture into h=113 bucket	V <sub>RF</sub> increases before extraction
Longitudinal emittance $6\pi\sigma_z\sigma_E$	0.20 eV-sec	0.20 eV-sec	2.60 eV-sec	4.08 eV-sec	2.76 eV-sec	2.76 eV-sec
$\sqrt{6}\sigma_z$	1.63 ns	9.42 ns	122 ns	8.89 ns	9.42 ns	5.5 ns
$\sqrt{6}\sigma_E$ ( $\sqrt{6}\sigma_E/E$ )	39.0 MeV ( $2.60 \times 10^{-4}$ )	8.31 MeV ( $5.54 \times 10^{-5}$ )	8.31 MeV ( $5.54 \times 10^{-5}$ )	114 MeV ( $7.61 \times 10^{-4}$ )	115 MeV ( $7.67 \times 10^{-4}$ )	160 MeV ( $1.06 \times 10^{-3}$ )
V <sub>RF</sub>	0.68 MV	2.30 kV	22 kV	22 kV	.438 MV	1.0 MV
h	1113	1113	53	53	1113	1113
$\gamma_s$	$1.51 \times 10^{-3}$	$8.72 \times 10^{-5}$	$5.91 \times 10^{-5}$	$5.91 \times 10^{-5}$	$1.21 \times 10^{-3}$	$1.83 \times 10^{-3}$
Number per bunch	$8 \times 10^9$	$8 \times 10^9$	$1.04 \times 10^{11}$	$1.04 \times 10^{11}$	$1 \times 10^{11}$	$1 \times 10^{11}$
Fast growth limits broad band $Z_H/n$	39.3 $\Omega$	10.3 $\Omega$	10.3 $\Omega$	141 $\Omega$	158 $\Omega$	176 $\Omega$
$Z_L$	366 M $\Omega$ /m	366 M $\Omega$ /m	366 M $\Omega$ /m	574 M $\Omega$ /m	404 M $\Omega$ /m	404 M $\Omega$ /m
narrow res. $Z_H/Q$	309 k $\Omega$	14.0 k $\Omega$	14.0 k $\Omega$	204 k $\Omega$	266 k $\Omega$	417 k $\Omega$
$Z_L/Q$	93.0 M $\Omega$ /m	19.8 M $\Omega$ /m	19.8 M $\Omega$ /m	20.9 M $\Omega$ /m	21.9 M $\Omega$ /m	30.5 M $\Omega$ /m
Slow growth limits $\bar{Z}_H/n$	222 $\Omega$	58.3 $\Omega$	58.3 $\Omega$	797 $\Omega$	894 $\Omega$	995 $\Omega$
$\bar{Z}_L$	103 M $\Omega$ /m	22.0 M $\Omega$ /m	22.0 M $\Omega$ /m	23.2 M $\Omega$ /m	24.4 M $\Omega$ /m	33.9 M $\Omega$ /m

Note: the fast growth broad band limits of  $Z_L$  are computed at 1.5 GHz

Table V. The first few transverse modes of a Main Ring bellow cavity

URMEL Mode number	Mode corr. to closed cavity	Resonance frequency (GHz)	Z/Q ( $\Omega$ )	Q	Z <sub>1</sub> /Q ( $\Omega$ /m)
ME1	TE <sub>111</sub> (1.55)	1.503	0.929	4855	22.64
EE1	TE <sub>112</sub> (2.66)	2.064	6.530	5513	115.91
ME2	TM <sub>111</sub> (2.56)	2.416	0.822	3927	12.47
EE2	TM <sub>110</sub> (2.72)	2.504	17.946	4795	262.58
EE3		2.801	2.272	5198	29.72
ME3		2.866	0.748	6081	9.56
ME4	TE <sub>113</sub> (3.09)	3.147	0.114	6216	1.33
EE4	TM <sub>112</sub> (3.18)	3.211	10.920	5445	124.60
ME5	TM <sub>113</sub> (3.82)	3.637	8.392	6767	84.54
EE5	TE <sub>114</sub> (3.98)	3.679	2.635	9825	26.24
ME6		3.696	9.214	6950	91.29

Note: Stainless steel with conductivity  $\sigma = 0.14 \times 10^7$  mho/m is used in the determination of Q. The fourth column shows the impedance per unit Q seen by a particle at a radius 3.61 cm from the center of the bellow. Both columns 4 and 6 are for one single bellow only.

Table VI. Total impedances of the Main Ring

	Low frequency average		Microwave region broad band ( $Z_H/n$ , $Z_L$ ) narrow resonance ( $Z_H/Q$ , $Z_L/Q$ )
	$Z_H/n$ ( $\Omega$ )	$Z_L$ (M $\Omega$ /m)	
Wall resistivity	1.01	3.51 (1.79)	
Lambertsons	0.23	0.52	$Z_H/n = 2.1 \Omega$ $Z_L = 0.47 \text{ M}\Omega/\text{m}$
Kickers	0.03	0.87	
Beam monitors	0.59	0.91	$Z_H/Q = 6.4 \text{ k}\Omega$ $Z_L/Q = 0.18 \text{ M}\Omega/\text{m}$
Bellows	2.46	1.32	$Z_H/Q = 37 \text{ k}\Omega$ $Z_L/Q = 0.26 \text{ M}\Omega/\text{m}$
Total	4.32	7.13 (5.29)	
Estimated limits (most stringent)	7.18	6.16	$Z_H/n = 1.3 \Omega$ $Z_L = 54 \text{ M}\Omega/\text{m}$ $Z_H/Q = 4.1 \text{ k}\Omega$ $Z_L/Q = 5.6 \text{ M}\Omega/\text{m}$

Note: Whenever the vertical and horizontal transverse impedances are different, the horizontal one is enclosed in brackets.

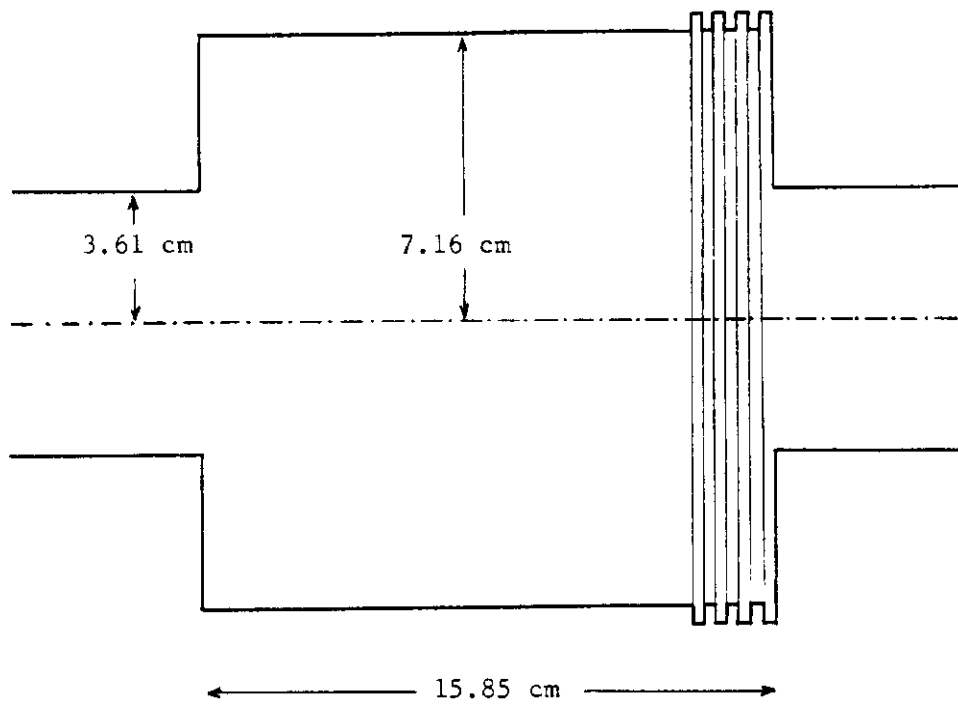


Figure 1. A typical Main Ring bellow

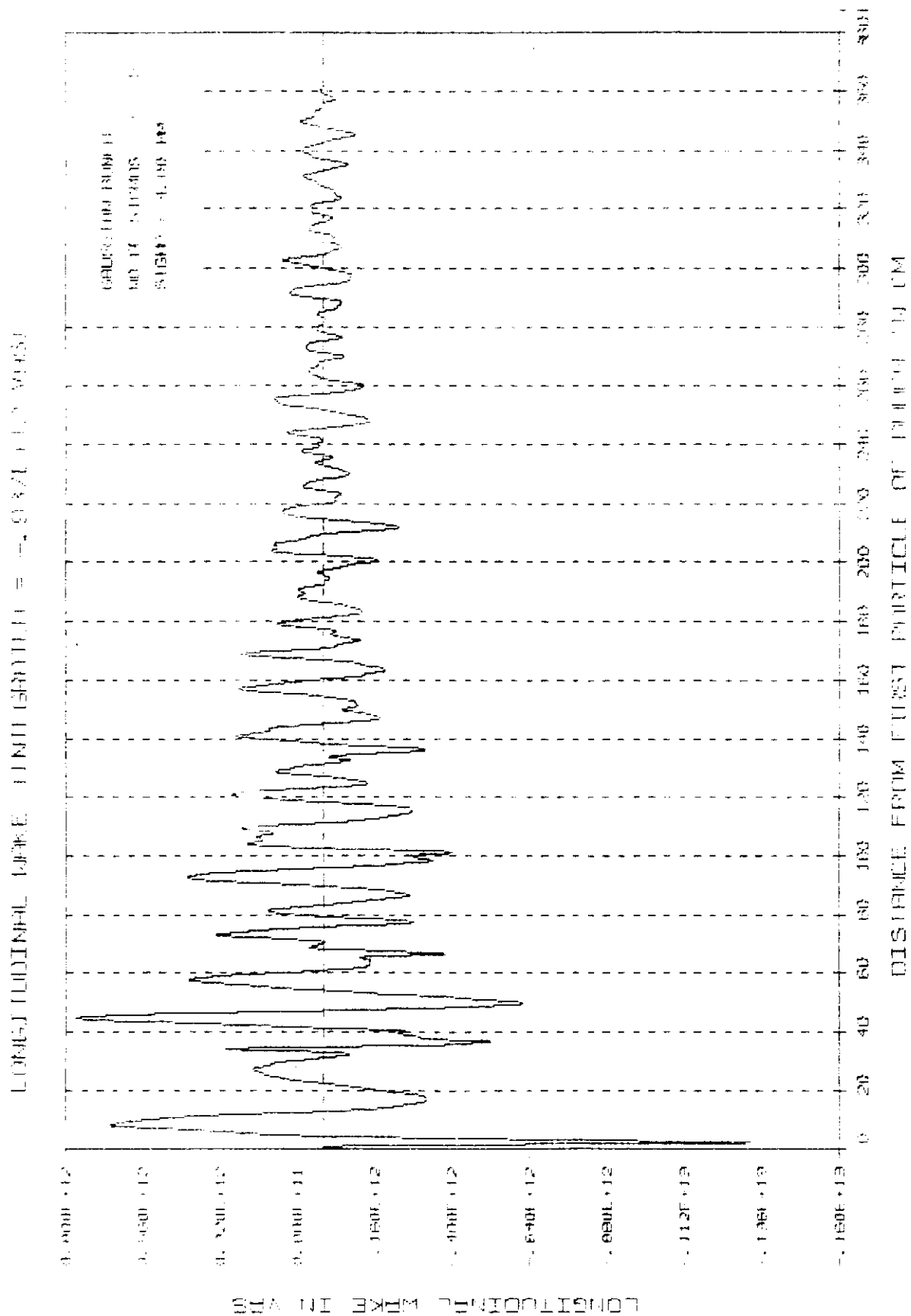


Figure 2. Longitudinal wake of a Main Ring bellow.

# LONGITUDINAL IMPEDANCE (REAL)

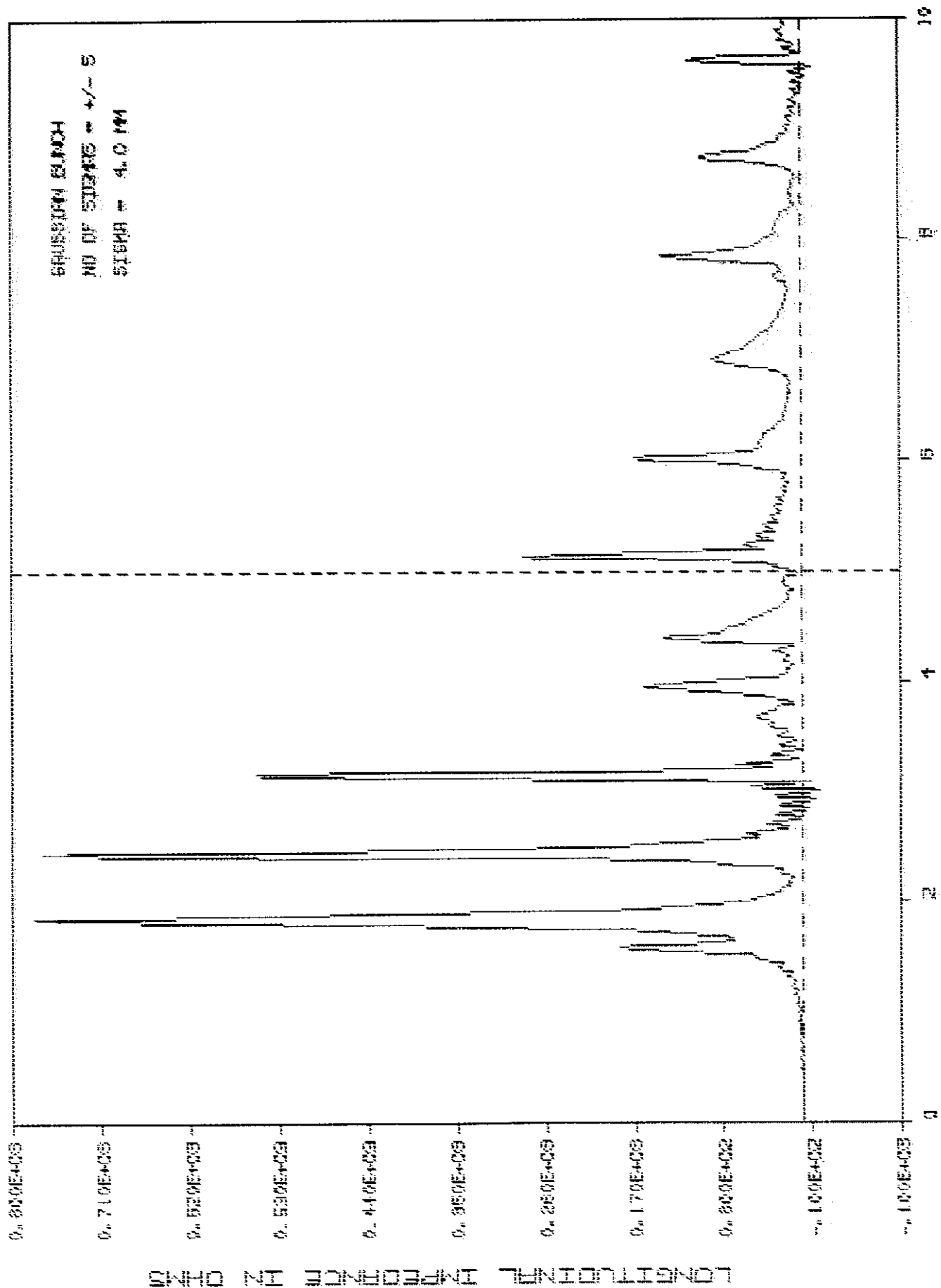


Figure 3.

# LONGITUDINAL IMPEDANCE (IMAGINARY)

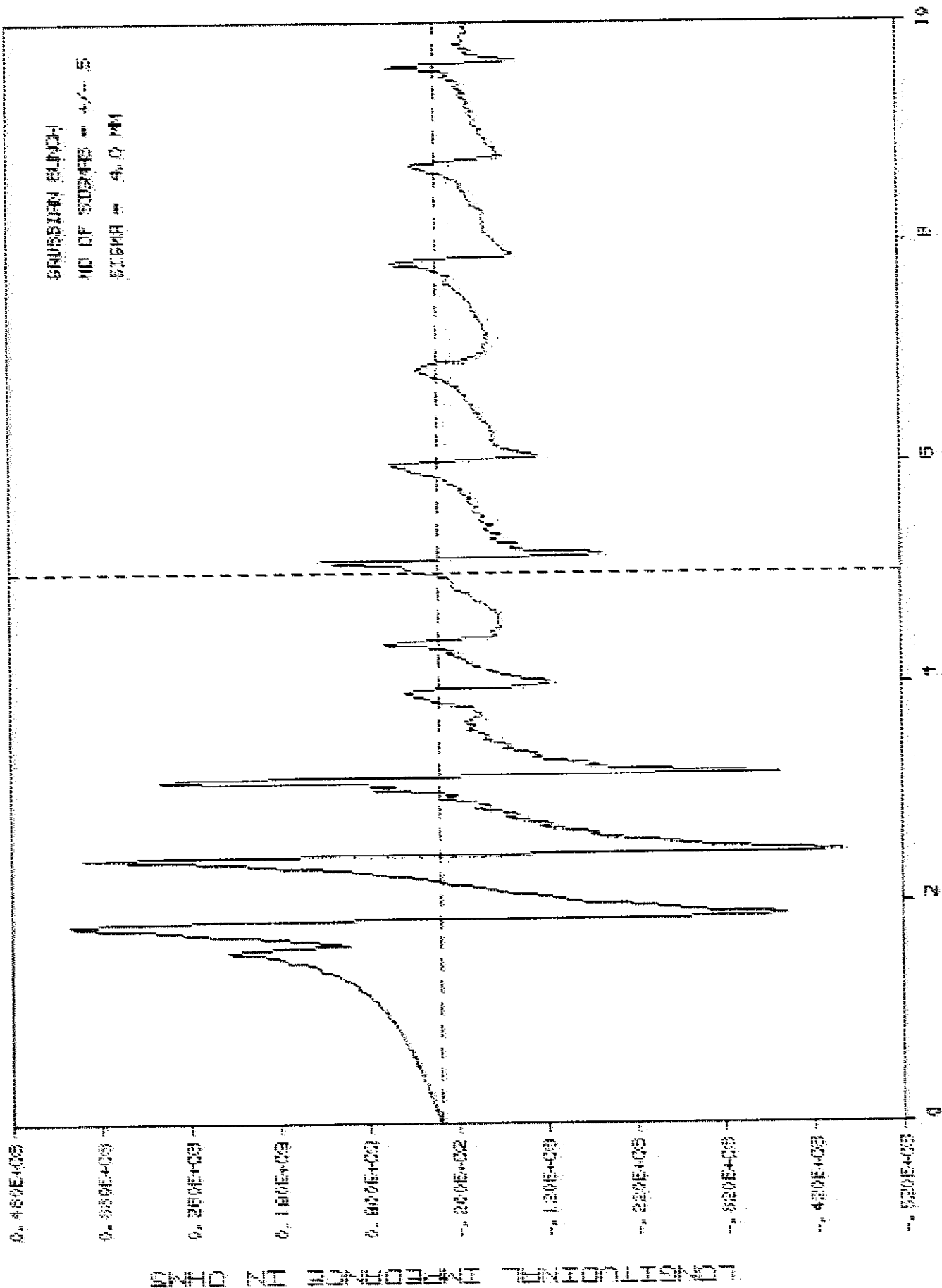


FIGURE 4



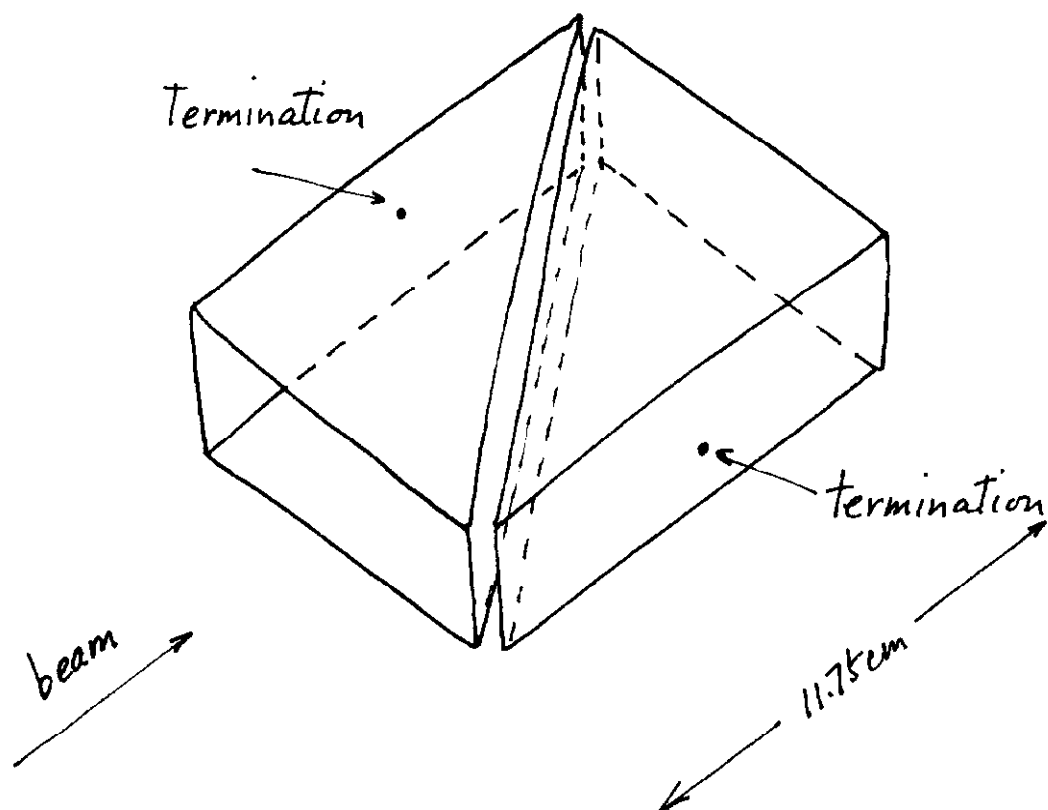


Figure 5. A beam monitor of the Main Ring.

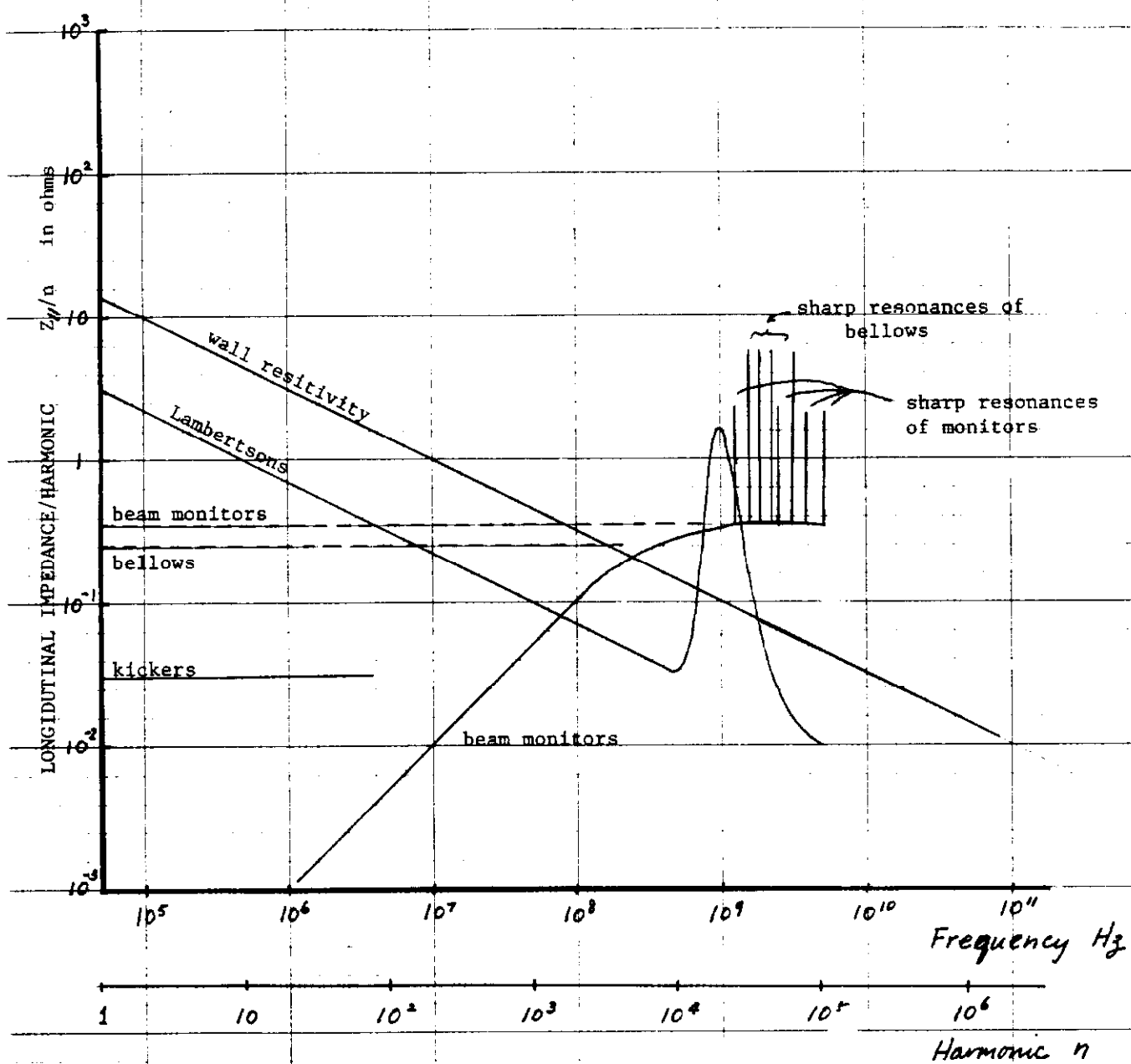


Figure 6. Longitudinal impedance per harmonic of the Main Ring. Solid curves are for real and dashed for inductive.

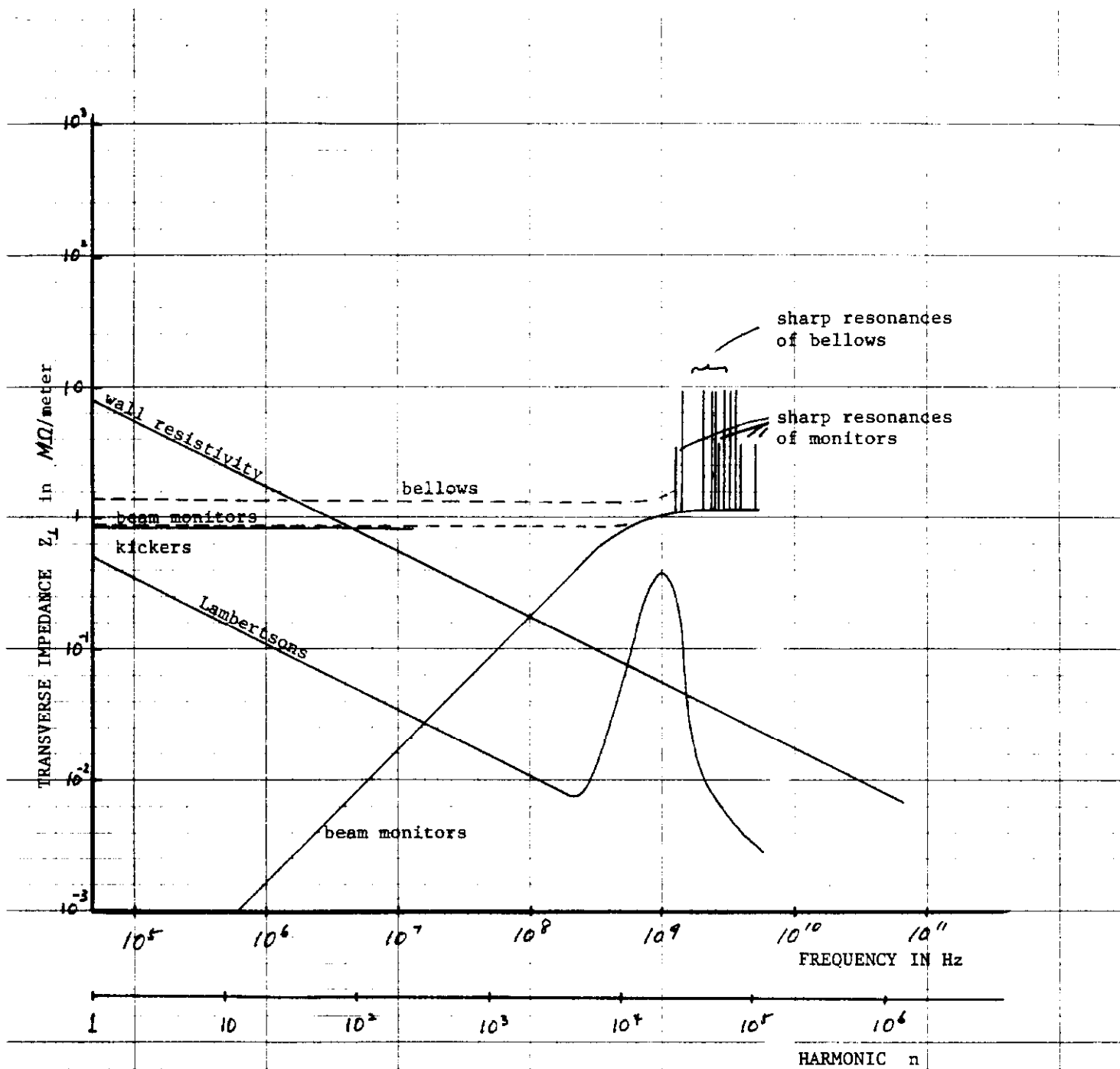


Figure 7. Transverse impedance of the Main Ring.  
Solid curves are for real and dashed for inductive.